Inorganic Materials, Vol. 37, No. 3, 2001, pp. 274–280. Translated from Neorganicheskie Materialy, Vol. 37, No. 3, 2001, pp. 342–348.
Original Russian Text Copyright © 2001 by Chekhomova.

Abrasive Properties of Modified Chromia

L. F. Chekhomova
Institute of Mechanical Engineering, Ural Division, Russian Academy of Sciences, Yekaterinburg, Russia

Received December 14, 1999; in final form, July 20, 2000

Abstract—ZrO_2-, CeO_2-, Y_2O_3-, La_2O_3-, and CaO-modified Cr_2O_3 abrasives were characterized by x-ray diffraction, electron microscopy, and sedimentation analysis. The results indicate the formation of solid solutions in narrow composition ranges. The materials offer a high abrasive ability and ensure residual roughness R_z = 0.04–0.09 μm in polishing precision parts of the ShKh-15 steel, with a product yield of up to 80–82%.

INTRODUCTION

Metal-oxide abrasives are used in final polishing stages to produce precision metal parts. The performance of abrasives depends on their chemical composition, particle-size distribution, and physicochemical and mechanical properties [1].

In addition, it is generally believed that the abrasive ability depends strongly on the chemical processes involved. The highest abrasive ability is offered by metal oxides with moderate hardness (Mohs' hardness in the range 6–7), including Cr_2O_3, which is tentatively attributed to the chemical interaction between the abrasive and the surface of the material being polished [2–5].

The performance of the common “soft” abrasives improves in the following order: $Al_2O_3 < ZrO_2 < Fe_2O_3 < Cr_2O_3 < CeO_2 \leq ThO_2$ [1]. Rare-earth oxides are of limited use because of the high cost but can be added to other abrasives as modifiers. The abrasive most widely used on a commercial scale is chromia, a relatively inexpensive material. However, Cr_2O_3 is not always capable of producing high-quality surfaces. Use is also made of Al_2O_3–Cr_2O_3 solid solutions, but these ensure product yields no higher than 50–55% [2, 3].

Thus, there is a need for improving the abrasive properties of Cr_2O_3. Equally important is the ability to reduce surface roughness by enhancing the reactivity of the abrasive, which would raise the product yield.

One way to raise the abrasive ability of Cr_2O_3 is to introduce modifiers. The most pronounced effect can be attained by using reactive elements which form solid solutions with Cr_2O_3, modifying its physicochemical properties (surface energy, particle size, and reactivity).

According to isomorphism theory [6–8], the main criterion for the formation of solid solutions is the cation–anion distance, determined by the sum of the ionic radii: the difference in atomic radius between the host cation and substituent should not exceed 15–20% (Goldschmidt's rule for ionic crystals and Hume-Rothery' rule for covalent crystals). At the same time, at high temperatures, solid solutions incorporating cations markedly different in size may be formed in a narrow composition range. In this context, it is important to locate the limits of solid solutions between Cr_2O_3 and oxides of larger sized cations.

Earlier work [9] showed that chromia may form chromites and solid solutions with rare-earth and calcium oxides. In particular, below 1600°C, the Cr_2O_3–CaO system contains mixed oxides with the general formula $m\text{MO} \cdot n\text{CrO}_3 \cdot p\text{Cr}_2\text{O}_3$ and the chromite $CaCr_2O_4$, which exists in two polymorphs: α (high-temperature) and β (low-temperature). The $\beta \longrightarrow \alpha$ phase transition occurs at 1570°C. The Cr_2O_3–ZrO_2 system contains Cr_2O_3-based rhombohedral and ZrO_2-based monoclinic solid solutions. According to phase-diagram data, the solid solution of ZrO_2 in Cr_2O_3 exists below 2000°C. In the Cr_2O_3–La_2O_3 system, $La_2O_3 \cdot Cr_2O_3$ and La_2O_3 form a eutectic with a melting point of 1380°C. Below this temperature, La_2O_3 and $LaCrO_3$ crystallize at Cr_2O_3 contents under 50 mol %. In the range 1000–1650°C, $LaCrO_3$ has a hexagonal structure [9].

Teruhisa *et al.* [10] and Peck *et al.* [11] reported the formation of $La_{1-x}Ca_xCrO_{3-\delta}$ ($x \leq 0.3$) perovskite solid solutions at ≃1000°C and studied the mechanism of Sr^{2+} substitution for Ca^{2+}. The only compound in the Cr_2O_3–Y_2O_3 system is the $YCrO_3$ perovskite, which forms eutectics with Y_2O_3 and Cr_2O_3. Zvereva *et al.* [12] obtained $YCaCr_xAl_{1-x}O_4$ solid solutions.

Thus, according to phase-diagram data [9], Cr_2O_3 is likely to form solid solutions with oxides of La, Y, Ce, Zr, and Ca between 1600 and 2000°C.

The purpose of this work was to study the effects that small amounts of ZrO_2, CeO_2, La_2O_3, Y_2O_3, and CaO modifiers have on the abrasive properties of Cr_2O_3.

EXPERIMENTAL

To modify chromia with CaO, ZrO_2, La_2O_3, Y_2O_3, and CeO_2 (≤0.18 mol %), mixtures of CrO_3 with $Ca(OH)_2$, $Zr(SO_4)_2$, La_2O_3, Y_2O_3, and $Ce(SO_4)_2$ were heat-treated first at 250°C for 1.5–2 h, then at 350–400°C for 1.0–1.5 h, and finally at 1000–1200°C for 1.5–2 h. This schedule was chosen with consideration for the mechanism of CrO_3 thermolysis [13].

X-ray diffraction (XRD) measurements were carried out on a DRON-2 powder diffractometer (CuK_α radiation) fitted with a UVD-2000 high-temperature attachment. Interplanar spacings were calculated by the centroid method. The lattice parameters of Cr_2O_3 and solid solutions were determined using the 110, 300, and $10\underline{10}$ lines with an accuracy of ±0.03, ±0.004, and ±0.002 Å, respectively. The volume of the hexagonal unit cell was calculated as $V = (3/2)^{1/2}(a^2c)$ [14] with an absolute uncertainty of ±0.3 $Å^3$. The lattice parameters were used to ascertain the formation of solid solutions. The lattice parameters of α-Cr_2O_3 were determined to be $a_0 = 4.955$ Å and $c_0 = 13.600$ Å, in agreement with earlier data [5, 15]. Chemical and phase analyses were carried out as described in [16] with a relative accuracy of ±0.001 mol %. Particle-size analysis was performed by gravity sedimentation using an SA-CP2 Shimadzu analyzer (viscosity of the dispersion medium, 9.3×10^{-4} Pa s; density of the liquid phase, 1.0 g/cm^3) and by electron microscopy (D-2 Carl Zeiss instrument).

Abrasive ability was assessed by a standard procedure using an S-15 polisher equipped with a sample holding fixture made of Bitumen 5. Four polished disks from the ShKh-15 quenched steel (HRC = 58–60) with $R_z = 0.3$–0.4 μm over a base length of 0.25 mm were fixed in the sample holder. Fine polishing was performed for 30 min at a load of 17.5 MPa. The rotation rates of the polishing wheel and the sample holder were 192 and 60 rpm, respectively. The polishing suspension was prepared from the modified Cr_2O_3 powder under investigation (25 g) and distilled water (175 ml). The material removal rate was calculated from weight loss data by the formula $P = \Delta M/(S\tau)$, where ΔM (mg) is the mean weight loss due to polishing, S (cm^2) is the sample surface area, and τ (min) is the polishing time. After polishing, the residual roughness R_z was determined as the average of ten measurements over a base length of 0.08 mm using an MII-4 optical microscope [17].

RESULTS AND DISCUSSION

According to XRD data, heat treatment of the $CrO_3 + Ca(OH)_2$, $CrO_3 + Zr(SO_4)_2$, $CrO_3 + Ca(OH)_2 + Zr(SO_4)_2$, $CrO_3 + La_2O_3$, $CrO_3 + Y_2O_3$, and $CrO_3 + Ce(SO_4)_2$ mixtures at the temperatures indicated above leads to CrO_3 decomposition into Cr_2O_3, possibly with the formation of solid solutions, through a number of intermediate compounds. The present results agree with earlier data [13, 18–21], except for some distinctions in the thermolysis products. The reaction sequence can be represented by the following schemes:

$$\overset{200\text{–}210^\circ C}{CrO_3(l)} + Ca(OH)_2 \xrightarrow{200\text{–}270^\circ C} CaCr_3O_{10}$$

$$+ Cr_2(Cr_{10}C_{31})_3 \xrightarrow{280^\circ C} CaCr_2O_7 + Cr_3O_8$$

$$+ Cr_2O_5 \xrightarrow{400^\circ C} CaCrO_4 + CrO_2 \xrightarrow{465^\circ C} CaCrO_4 \qquad (I)$$

$$+ CrO_{1.56} \xrightarrow{900\text{–}1200^\circ C} Cr_{2-x}Ca_xO_{3-\delta} + CaCr_2O_4 + O_2,$$

$$\overset{200\text{–}210^\circ C}{CrO_3(l)} + Zr(SO_4)_2 \xrightarrow{280\text{–}300^\circ C} Cr_2(Cr_{10}O_{31})_3$$

$$+ Zr_2(OH)_2SO_4(CrO_4)_2$$

$$\xrightarrow{360\text{–}370^\circ C} Zr_2(OH)_2SO_4(CrO_4)_2$$

$$+ Cr_2(Cr_2O_7)_3 \xrightarrow{440^\circ C} Zr_2(OH)_2SO_4(CrO_4)_2 \qquad (II)$$

$$+ Cr_2(CrO_4)_3 \xrightarrow{465^\circ C} CrO_{1.56}$$

$$+ Zr_2(OH)_2SO_4(CrO_4)_2 \xrightarrow{1000\text{–}1100^\circ C} Cr_{2-x}Zr_xO_{3+\delta}$$

$$+ ZrO_2 + SO_2,$$

$$\overset{200\text{–}210^\circ C}{CrO_3(l)} + Zr(SO_4)_2$$

$$+ Ca(OH)_2 \xrightarrow{280\text{–}300^\circ C} Cr_2(Cr_{10}O_{31})_3$$

$$+ Zr_2(OH)_2SO_4(CrO_4)_2$$

$$+ CaCr_2O_7 \xrightarrow{350\text{–}370^\circ C} Zr_2(OH)_2SO_4(CrO_4)_2$$

$$+ Cr_2(Cr_2O_7)_3 + CaCr_2O_7 \xrightarrow{440^\circ C} Cr_2(CrO_4)_3 \qquad (III)$$

$$+ CaCrO_4 + Zr_2(OH)_2SO_4(CrO_4)_2 \xrightarrow{465^\circ C} CrO_{1.56}$$

$$+ Zr_2(OH)_2SO_4(CrO_4)_2$$

$$+ CaCrO_4 \xrightarrow{1000\text{–}1100^\circ C} Cr_{2-x_1-x_2}Zr_{x_1}Ca_{x_2}O_{3-\delta}$$

$$+ ZrO_2 + Zr(OH)_2CrO_4 + SO_2,$$

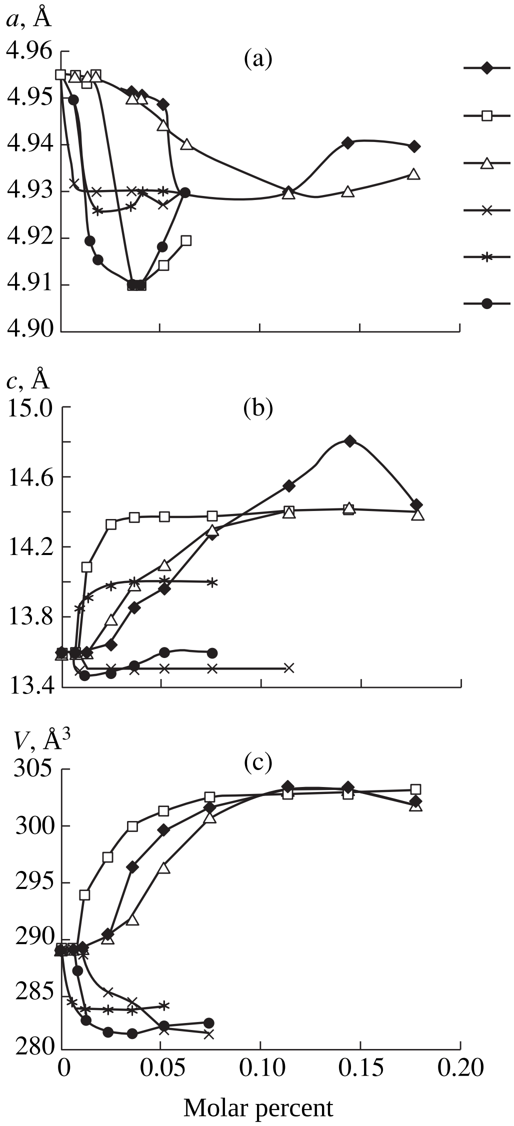

Fig. 1. Composition dependences of lattice parameters for Cr_2O_3 modified with (*1*) CaO, (*2*) ZrO_2, (*3*) CaO + ZrO_2 (2 : 1), (*4*) La_2O_3, (*5*) Y_2O_3, and (*6*) CeO_2.

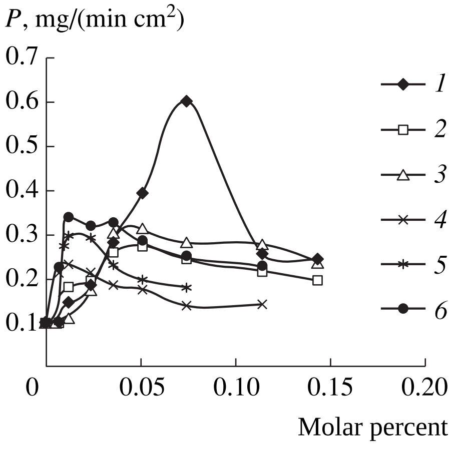

Fig. 2. Composition dependences of abrasive ability for modified Cr_2O_3: (*1*–*6*) same as in Fig. 1.

$$CrO_3 + La_2O_3 \xrightarrow{200–250°C} Cr_2(Cr_{10}O_{31})_3$$

$$+ La_2(Cr_2O_7)_3 \xrightarrow{350–370°C} Cr_2(Cr_2O_7)_3$$

$$+ La_2(CrO_4)_3 \xrightarrow{465°C} CrO_{1.56} \qquad \text{(IV)}$$

$$+ La_2(CrO_4)_3 \xrightarrow{600–660°C} LaCrO_4 + Cr_2O_3$$

$$+ O_2 \xrightarrow{750°C} LaCrO_3 + Cr_2O_3 \xrightarrow{1000–1100°C} Cr_{2-x}La_xO_3,$$

$$\overset{200–210°C}{CrO_3} + Y_2O_3 \xrightarrow{200–250°C} Cr_2(Cr_{10}O_{31})_3$$

$$+ Y_2(Cr_2O_7)_3 \xrightarrow{456°C} Y_2(CrO_4)_3$$

$$+ CrO_{1.56} \xrightarrow{560–600°C} YCrO_4 + Cr_2O_3 \qquad \text{(V)}$$

$$+ O_2 \xrightarrow{740°C} YCrO_3$$

$$+ Cr_2O_3 \xrightarrow{900–1100°C} YCrO_3 + Cr_{2-x}Y_xO_3,$$

$$\overset{200–210°C}{CrO_3(l)} + Ce(SO_4)_2 \xrightarrow{280–300°C} Cr_2(Cr_{10}O_{31})_3$$

$$+ Ce_2(OH)_2SO_4(CrO_4)_2 \xrightarrow{350–370°C} Cr_2(Cr_2O_7)_3$$

$$+ Ce_2(OH)_2SO_4(CrO_4)_2 \xrightarrow{450°C} Cr_2(CrO_4)_3$$

$$+ Ce_2(OH)_2SO_4(CrO_4)_2 \qquad \text{(VI)}$$

$$\xrightarrow{465°C} Ce_2(OH)_2SO_4(CrO_4)_2$$

$$+ CrO_{1.56} \xrightarrow{900–1100°C} Cr_{2-x}Ce_xO_{3+\delta}$$

$$+ CeO_2 + CeOCrO_4 + SO_2.$$

The data displayed in Fig. 1 demonstrate that *a* decreases with increasing modifier content in the ranges 0–0.10 mol % CaO and 0–0.05 mol % ZrO_2, La_2O_3, Y_2O_3, and CeO_2; *c* and *V* increase with modifier content in the same composition ranges. The lattice parameters of the La_2O_3-, Y_2O_3-, and CeO_2-modified materials decrease by 3–4% in the range 0–0.03 mol %.

The observed variations of lattice parameters suggest that the Zr^{4+}, La^{3+}, Y^{3+}, Ce^{4+}, and Ca^{2+} ions substitute for Cr^{3+}. In the case of Zr^{4+} and Ca^{2+}, the difference in charge state and ionic radius between the substituent and Cr^{3+} leads to the formation of a defective lattice and an increase in unit-cell volume, which testifies to a reduction in atomic density and an increase in Cr_2O_3 reactivity. The abrasive abilities of the CaO- and

ZrO_2-containing materials vary with modifier content in a similar way (Fig. 2).

The observed variations of the abrasive ability with modifier content are not surprising. According to Hauffe [22], substitutions at the Cr site and Cr^{3+} deficiency reduce atomic density. The highest abrasive ability was shown by Cr_2O_3 modified with 0.04–0.09 mol % CaO (3–6 times higher in comparison with Cr_2O_3). Note that the increase in abrasive ability is likely due to the formation of solid solutions, since, with increasing calcium chromite content (0.12–0.18 mol % CaO), the abrasive ability decreases to the level typical of pure Cr_2O_3.

In the case of Cr_2O_3 modified with 0.02–0.035 mol % CaO, the residual roughness was $R_z = 0.10$ μm (Fig. 3). The largest R_z (0.17–0.19 μm) was observed at 0.05–0.09 mol % CaO.

Solid solutions can be formed by two mechanisms. If the oxygen stoichiometry remains unchanged, some of the Ca^{2+} ions are incorporated interstitially to give the $Cr_{2-x}Ca_{1.5x}O_3$ solid solution, in which one Cr ion is replaced by 1.5 Ca ions. This mechanism is however unlikely in view of the large ionic radius of Ca. In the second mechanism, the cation stoichiometry remains unchanged, and the solid solution contains oxygen vacancies, as described by the formula $Cr_{2-x}Ca_xO_{3-\delta}$, with $0 \le \delta \le 0.045$.

According to sedimentation analysis and electron microscopy data, the introduction of Ca^{2+} ions increases the particle size of Cr_2O_3 from 0.5–1 to 3–5 μm (Figs. 4, 5). As the CaO content rises from 0.04 to 0.09 mol %, the particle size gradually increases to d = 1–4 μm, the most probable size range being 1–2 μm. A small fraction of the particles fall in the range d = 0.2–0.5 μm.

The introduction of Zr^{4+} ions increases the abrasive ability to P = 0.24–0.27 mg/(min cm^2) and reduces the residual roughness to R_z = 0.07–0.09 μm (Figs. 2, 3). The major size range in ZrO_2-modified Cr_2O_3 is 1–2 μm; particles with d = 2–5 μm are also present. At the same time, the fraction of fine particles with d in the range 0.4–1 μm increases. The increase in the abrasive ability is attributable to the formation of $Cr_{2-x}Zr_xO_{3+\delta}$ solid solutions with $0 < x \le 0.04$ and $0 \le \delta \le 0.02$.

$CaO + ZrO_2$ additions are, most likely, incorporated substitutionally, yielding $Cr_{2-x_1-x_2}Zr_{x_1}Ca_{x_2}O_{3-\delta}$ oxygen-deficient solid solutions with $0 < x_1 \le 0.04$, $0 < x_2 \le 0.09$, and $0 < \delta \le 0.025$. The material also contains pseudocubic ZrO_2 and zirconium hydroxochromate, $Zr(OH)_2CrO_4$, as evidenced by the XRD peaks with d = 3.48 (100% intensity), 2.93 (60%), 2.84 (50%), 1.807 (39%), and 1.574 Å (30%), in agreement with an earlier report that $Zr(OH)_2CrO_4$ forms at 140–190°C and is stable up to 1200°C [23]. The highest abrasive ability, 0.28–0.34 mg/(min cm^2), is observed in the range 0.04–0.09 mol % CaO + 0.02–0.04 mol % ZrO_2 (Fig. 2, curve *3*), where the lattice parameters vary substantially. The residual roughness attained with these compositions is R_z = 0.08–0.09 μm (Fig. 3, curve *3*).

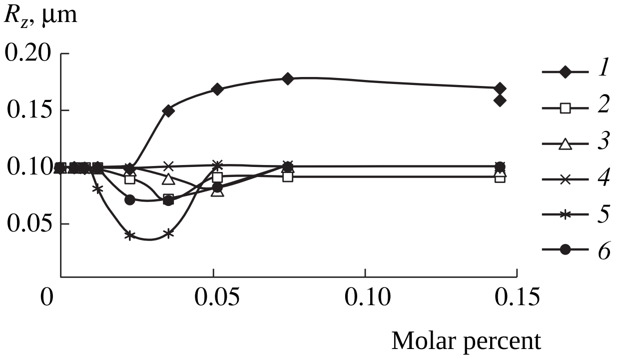

Fig. 3. Composition dependences of residual roughness for modified Cr_2O_3: (*1–6*) same as in Fig. 1.

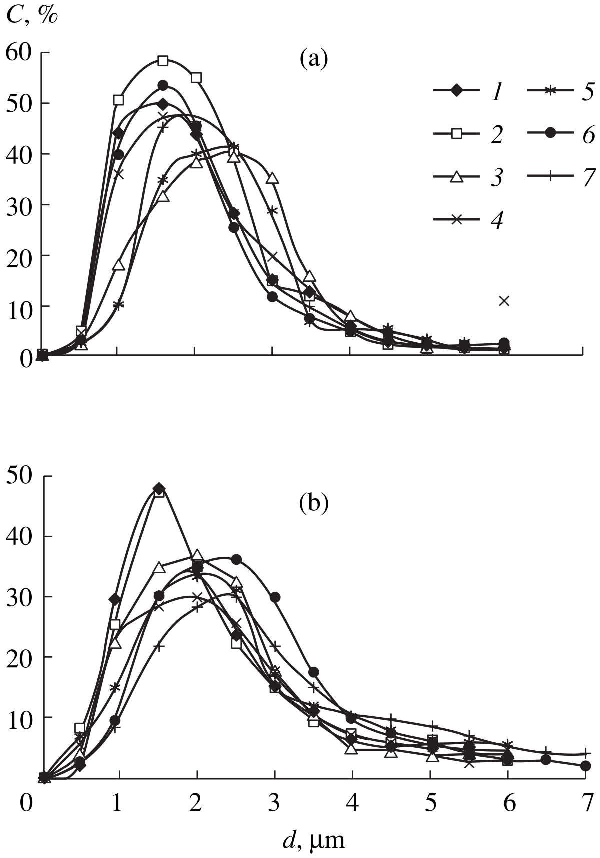

Fig. 4. Particle-size distributions of modified Cr_2O_3 containing (a) (*1*) 0, (*2*) 0.05, (*3*) 0.06, (*4*) 0.07, (*5*) 0.08, (*6*) 0.09, and (*7*) 0.18 mol % CaO and (b) (*1*) 0.02–0.05 + 0.02, (*2*) 0.03 + 0.02, (*3*) 0.04 + 0.03, (*4*) 0.05 + 0.05, (*5*) 0.03 + 0.05, (*6*) 0.08 + 0.04, and (*7*) 0.07 + 0.05 mol % $CaO + ZrO_2$.

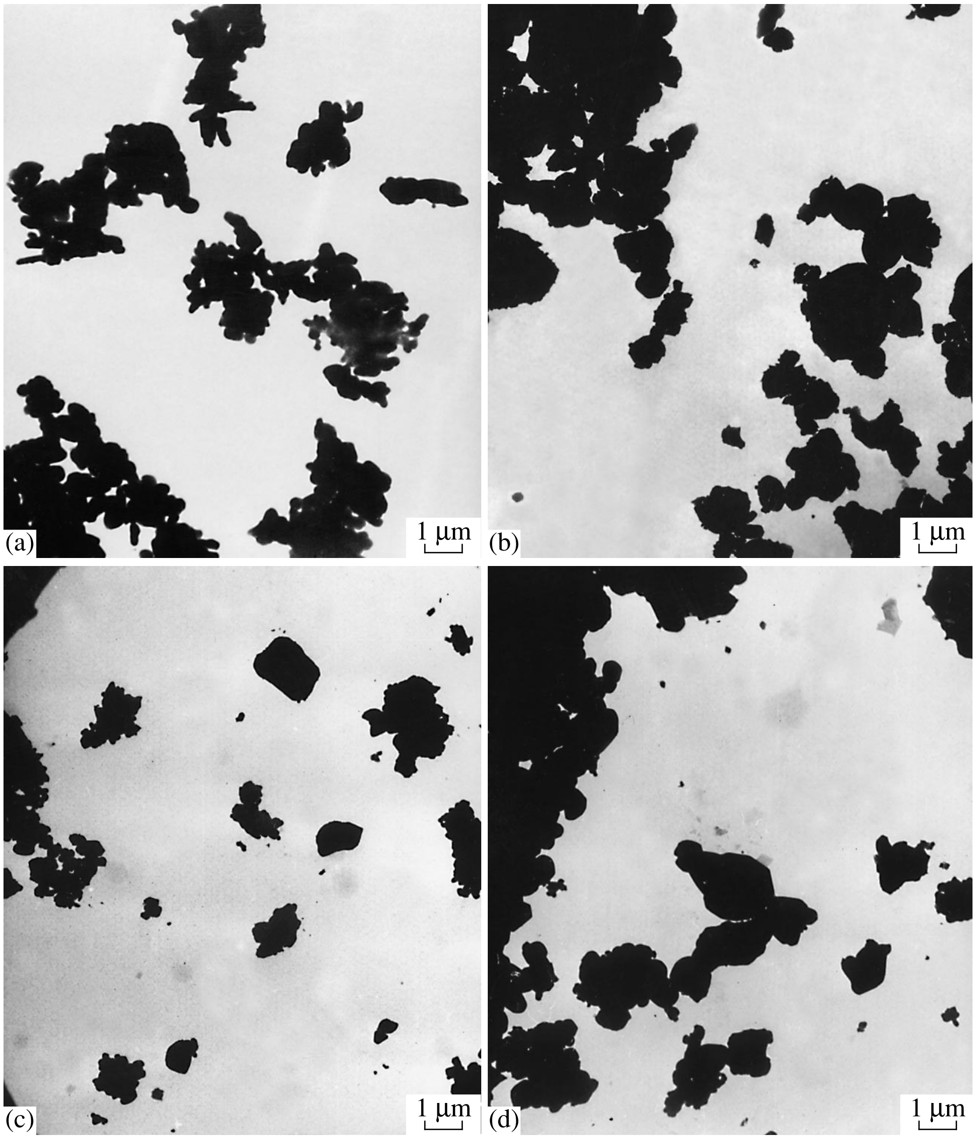

Fig. 5. Electron micrographs of (a) Cr_2O_3, (b) Cr_2O_3 + 0.05 mol % CaO; (c) Cr_2O_3 + 0.02 mol % ZrO_2, and (d) Cr_2O_3 + 0.04 mol % CaO + 0.02 mol % ZrO_2; ×6000.

Cr_2O_3 modified with Ca^{2+} and Zr^{4+} ions was found to contain, along with particles 2–5 μm in size, fine particles with d from 0.04 to 0.50 μm, which are likely to ensure a high quality of polished metal surfaces (Figs. 3, 4b, 5d).

The composition dependence of the lattice parameters for La_2O_3-modified Cr_2O_3 indicates the formation of $Cr_{2-x}La_xO_3$ solid solutions in the composition range $0 < x \leq 0.018$, where the abrasive ability increases twofold. The residual roughness is 0.10 μm (Fig. 3, curve *4*). The major size range is 1–2 μm. As the La_2O_3 content increases from 0.02 to 0.05 mol %, the particle size increases to 3–4 μm, as supported by sedimentation analysis (Fig. 6a).

The introduction of Y^{3+} ions increases the abrasive ability of Cr_2O_3 by a factor of 3 (Fig. 2, curve *5*) and reduces R_z to 0.04–0.07 μm, which can be accounted for by the formation of $Cr_{2-x}Y_xO_3$ solid solutions with $0 < x \leq 0.026$. The powders modified with 0.01–0.03 mol % Y_2O_3 range in particle size from 0.05–0.5 to 5–6 μm (Fig. 6b).

Ce^{4+} ions raise the abrasive ability of Cr_2O_3 to 0.30–0.32 mg/(min cm^2), ensuring R_z = 0.07–0.09 μm. The composition dependences of lattice parameters in the Cr_2O_3–CeO_2 system indicate the formation of $Cr_{2-x}Ce_xO_{3+\delta}$ heterovalent substitutional solid solutions with $0 < x \leq 0.03$ and $0 < \delta \leq 0.15$. In addition, the CeO_2-modified materials contain $CeOCrO_4$ [24]. The

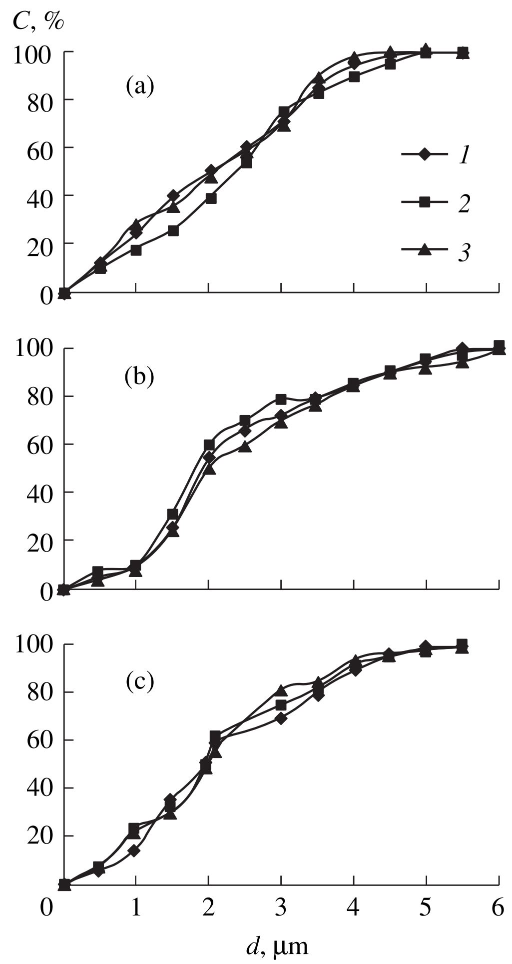

Fig. 6. Cumulative particle-size distributions of modified Cr_2O_3 containing (a) (*1*) 0.02, (*2*) 0, and (*3*) 0.05 mol % La_2O_3; (b) (*1*) 0.01, (*2*) 0.03, and (*3*) 0.04 mol % Y_2O_3; and (c) (*1*) 0.02, (*2*) 0.03, and (*3*) 0.06 mol % CeO_2.

powders consist of both coarse (4–5 μm) and fine (<0.5 μm, 5–8 wt %) particles (Fig. 6c).

CONCLUSION

The present results demonstrate that the abrasive ability of Cr_2O_3 modified with rare-earth oxides and CaO and the residual roughness correlate with the observed variations in lattice parameters, indicating the formation of solid solutions. The introduction of these modifiers raises the abrasive ability of Cr_2O_3 by a factor of 3–6. The lowest residual roughness, R_z = 0.04–0.09 μm, is attained with the ZrO_2, Y_2O_3, CeO_2, and CaO + ZrO_2 modifiers, which is attributable to the presence of both coarse and fine particles, the latter exhibiting high reactivity in the polishing process. The modified Cr_2O_3 abrasives ensure a product yield of 80–82% in polishing precision metal parts.

REFERENCES

1. Garshin, A.P., Gropyanov, V.M., and Lagunov, Yu.V., *Abrazivnye materialy* (Abrasives), Leningrad: Mashinostroenie, 1983.
2. Getts, I., *Shlifovka i polirovka stekla* (Grinding and Polishing of Glass), Leningrad: Stroiizdat, 1967.
3. Dubrovskii, V.A., Colloid-Chemical Processes in Glass Polishing, *Opt.–Mekh. Prom–st.*, 1956, no. 2, pp. 52–58.
4. Vinokurov, A.P., *Issledovanie protsessa polirovaniya stekla* (Polishing of Glass), Moscow: Mashinostroenie, 1967.
5. Viktorov, V.V., Fotiev, A.A., and Badich, V.D., Abrasive and Thermal Properties of Al_2O_3–Cr_2O_3 Solid Solutions, *Neorg. Mater.*, 1996, vol. 32, no. 1, pp. 63–65 [*Inorg. Mater.* (Engl. Transl.), vol. 32, no. 1, pp. 55–57].
6. Kitaigorodskii, A.I., *Smeshannye kristally* (Mixed Crystals), Moscow: Nauka, 1983.
7. Urusov, V.S., *Teoreticheskaya kristallokhimiya* (Theoretical Crystal Chemistry), Moscow: Mosk. Gos. Univ., 1987.
8. Makarov, E.S., *Izomorfizm atomov v kristallakh* (Isomorphism of Atoms in Crystals), Moscow: Nauka, 1973.
9. *Diagrammy sostoyaniya sistem tugoplavkikh oksidov: Spravochnik. Vyp. 5: Dvoinye sistemy* (Phase Diagrams of Refractory Oxide Systems, issue 5: Binary Systems), Leningrad: Nauka, 1988, parts 1, 4.
10. Horita Teruhisa, Sakai Natsuko, Yokokawa Harumi, and Dokiya Masayuki, Grain-Boundary Diffusion of Strontium in (La,Ca)CrO_3 Perovskite-Type Oxide by SIMS, *J. Am. Ceram. Soc.*, 1998, vol. 81, no. 2, pp. 315–320.
11. Peck, D.H., Miler, M., and Hilpert, K., Phase Diagram Study in the CaO–Cr_2O_3–La_2O_3 System in Air and under Low Oxygen Pressure, *Solid State Ionics*, 1999, vol. 123, nos. 1–4, pp. 47–57.
12. Zvereva, I.A., Anashkina, N.F., and Chezhina, N.V., Magnetochemical Study of $YCaCr_xAl_{1-x}O_4$ Solid Solutions, *Vestnik Leningr. Univ., Ser. 4: Fiz., Khim.*, 1991, no. 1, pp. 108–110.
13. Rode, T.V., *Kislorodnye soedineniya khroma i khromovye katalizatory* (Chromium Oxide Compounds and Chromium Catalysts), Moscow: Akad. Nauk SSSR, 1962.
14. Kachanov, N.N. and Mirkin, L.I., *Rentgenostrukturnyi analiz (polikristallov)* (X-ray Diffraction Analysis of Polycrystals), Moscow: Nauchno-Tekh. Izd. Mashinostroitel’noi Literatury, 1960.
15. *Neorganicheskie soedineniya khroma: Spravochnik* (Inorganic Chromium Compounds: A Handbook), Ryabin, V.A. *et al.*, Eds., Leningrad: Khimiya, 1981.
16. Knipovich, Yu.N. and Morachevskii, Yu.V., *Analiz mineral’nogo syr’ya* (Analysis of Mineral Raw Materials), Leningrad, 1959.
17. *GOST* (State Standard) *2912-88: Commercial Chromium Oxide*, 1988.
18. Pavlikov, V.M., Shevchenko, A.V., and Lopato, L.M., Rare-Earth Chromites and Their Physicochemical Properties, *Trudy II Vsesoyuznogo soveshchaniya po khimii okislov pri vysokikh temperaturakh* (Proc. II All-Union

Conf. on the High-Temperature Chemistry of Oxides), Leningrad, 1967, pp. 52–58.

19. Suvorov, S.A. and Nikiforov, A.Yu., Synthesis, Phase Transitions, and Electrical Properties of Lanthanum-Chromite-Based Ceramic-Matrix Composites, *Zh. Prikl. Khim.*, 1991, no. 2, pp. 469–473.
20. Zakharova, N.D., Zhitkova, T.N., Kalitina, L.N., *et al.*, Phase Transformations in the Preparation of Lanthanum Chromate(III), *Tr. Ural. Nauchno-Issled. Khim. Inst.*, 1991, no. 69, pp. 93–95.
21. Zakharova, N.D., Ryabin, V.A., Leont'eva, I.A., and Zhitkova, T.N., Thermal Decomposition of Yttrium Chromates, *Tr. Ural. Nauchno-Issled. Khim. Inst.*, 1981, no. 52, pp. 46–49.
22. Hauffe, K., *Reaktionen in und an festen Stoffen*, Berlin: Springer, 1955. Translated under the title *Reaktsii v tverdykh telakh i na ikh poverkhnosti*, Moscow: Inostrannaya Literatura, 1962.
23. Wanda, M., The Crystal Structure of $Zr_4(OH)_6(CrO_4)_5H_2O$, *Acta Chem. Scand.*, 1973, vol. 27, pp. 177–190.
24. *Powder Diffraction File*, Swarthmore: Joint Committee on Powder Diffraction Standards.